JACS
JOURNAL OF THE AMERICAN CHEMICAL SOCIETY

Communication

pubs.acs.org/JACS

From 3-Fold Completive Self-Sorting of a Nine-Component Library to a Seven-Component Scalene Quadrilateral

Manik Lal Saha and Michael Schmittel*

Center of Micro and Nanochemistry and Engineering, Organische Chemie I, Universität Siegen, Adolf-Reichwein-Straße 2, D-57068 Siegen, Germany

Supporting Information

ABSTRACT: Three-fold completive self-sorting of a nine-component library with ≥126 possible combinations led to the clean formation of only three heteroleptic metal−ligand complexes. Due to the orthogonality of the latter, they were used as corner stones in an integrative self-sorting approach toward a seven-component scalene quadrilateral.

Multicomponent self-assembly is a key protocol in biology to generate intricate systems ranging from viral capsids to cells as the functional basis of life itself.[1] In this *modus operandi*, Nature efficiently combines self-assembly/self-organization and self-sorting[2] to ensure correct stoichiometric and proper spatial/positional arrangement in the final structure, as otherwise the desired function will not emerge.[3] Increasing the degree of self-sorting[2d] in metallo-supramolecular heteroassembly is thus extremely valuable as it leads the way to functional aggregates with each component possibly adding new functions. Such an approach requires supreme managing of "order-out-of-chaos"[4] protocols, i.e., formation of a single assembly from a pool of communicative[5] ligands and metal ions, without wasting any constituent. Clearly, in arrangements with increasing number of components, detrimental cross-talk[5b] will increase rapidly, unless a high level of molecular programming is implemented.[6] At present, the state-of-the-art examples for abiological multicomponent self-assembly[7] comprise at most four[8,9] or five different components.[10] Exceeding those boundaries, we describe herein a nine-component 3-fold completive[2d] self-sorted library (Scheme 1a) and elaborate from there the clean formation of the seven-component scalene quadrilateral **QL** (Scheme 1b,c) using two metal ions and five ligands. For the first time, a dynamic 2D metallomacrocycle encompasses seven distinct components in its framework.

Over the years, we have refined two protocols toward heteroleptic complexes, the HETPHEN (heteroleptic bisphenanthroline complexes) and HETTAP (heteroleptic terpyridine and phenanthroline complexes) methods,[11] and demonstrated their utility in constructing a large number of dynamic supramolecular structures.[12] Using the HETPHEN strategy in combination with insight from Nitschke,[13] we recently developed a HETPHEN variant for engineering constitutionally dynamic heteroleptic complexes of the type [Cu(**1**)(iminopyridine)]$^+$, such as **C1** from its precursor complex [Cu(**1**)(**2**)]$^+$ (Scheme 1a).[14] Here, the [Cu(**1**)]$^+$ ion acts as both catalyst and binding glue to the emergent iminopyridine ligand thereby driving its formation to completion.[14a] Extending the above strategy toward *in situ* formation of analogous HETTAP-based diiminopyridine complexes required

Scheme 1. (a) Generation of Three Orthogonal Complexes from a Nine-Component Completive Self-Sorting Library; (b) Chemical Structures of Ligands 8−13; and (c) Integrative Self-Sorting Synthesis of Scalene Quadrilateral QL

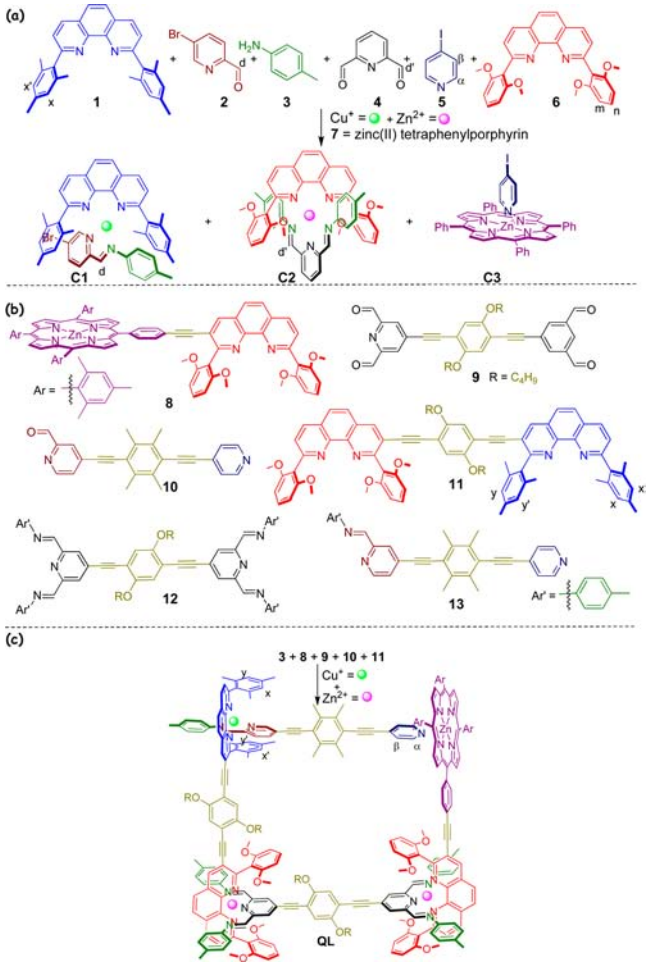

Received: October 10, 2013
Published: November 13, 2013

   dx.doi.org/10.1021/ja410425k | J. Am. Chem. Soc. 2013, 135, 17743−17746

Scheme 2. Optimization of the Parallel Formation of Bis(iminopyridine)s and Their HETTAP Complexes

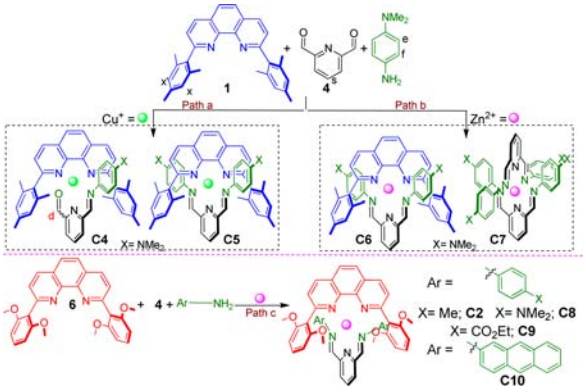

extensive optimization, as demonstrated in Scheme 2, paths a–c. For example, $[Cu(\mathbf{1})]^+$ as template failed to sustain full diimine formation at **4** (Scheme 2, path a) due to the preference of Cu^+ ions for coordination number 4 rather than 5 (see Figures S22 and S40).[15] In contrast, the higher charged $[Zn(\mathbf{1})]^{2+}$ (Scheme 2, path b) supported diimine formation at **4**, but additionally led to formation of the undesired hexacoordinated complex[16] **C7** (~15%, based on ^{1}H NMR, see Figures S23 and S42) aside of **C6**. Earlier studies indicated that the overall association constant β for HETTAP complexes is substantially altered by varying its sterically shielded counterpart. For example, complexes of type $[Zn(\mathbf{6})(terpy)]^{2+}$ ($\log \beta \approx 14$) are thermodynamically more stable than those of type $[Zn(\mathbf{1})(terpy)]^{2+}$ ($\log \beta \approx 12$).[17] To enforce HETTAP complexation, we thus selected 2,9-bis(2,6-dimethoxyphenyl)-1,10-phenanthroline (**6**), a pseudo-tridentate ligand due to its methoxy groups.[10] Indeed, complexes **C2**, **C8**–**C10** (Scheme 2, path c) were quantitatively afforded from a 1:1:1:2 mixture of **6**, **4**, Zn^{2+}, and the respective amines and fully characterized by ^{1}H NMR, ^{13}C NMR, electrospray ionization mass spectroscopy (ESI-MS), IR, and elemental analysis (see SI). In addition, the crystal structure of **C10**, though poorly resolved, clearly demonstrated the distorted octahedral geometry at the central zinc(II) ion with one coordination site being filled at ~2.4 Å distance by one of the oxygen atoms of ligand **6** (see Figures S48 and S49). It is noteworthy that in contrast to the facile formation of HETPHEN-like complex $[Cu(\mathbf{1})(\mathbf{2})]^+$ that readily undergoes imine formation in presence of **3**,[14a] the weakly binding pyridine-2,6-dicarbaldehyde (**4**) failed to yield the HETTAP complex $[Zn(\mathbf{6})(\mathbf{4})]^{2+}$ due to preferential formation of $[Zn(\mathbf{6})_2]^{2+}$. Evidently, the 2,6-dimethoxyphenyl groups in **6** are not sufficiently bulky to prevent formation of the rather stable $[Zn(\mathbf{6})_2]^{2+}$ (see Figures S24 and S41).[18]

Considering the insight from the experiments above, we reasoned that self-sorting of complexes **C1** and **C2** (Scheme 1a) could serve as a blueprint for completive self-sorting[2d] as their choice for distinct phenanthroline counterparts is firmly guided by metal-coordination specifics. Indeed, 2-fold completive self-sorting of **C1** and **C2** is nicely proven by ^{1}H NMR (Figure 1c) and ESI-MS (see Figure S44). As a third non-interfering complexation unit we turned to the pyridine–zinc(II) porphyrin binding motif **C3**, as we had recently established its modulated orthogonality[5b] with both HETPHEN and HETTAP complexes[10] by exploiting maximum site occupancy[19] and steric costs. In particular, steric bulk at the bi- or tridentate ligands is the key to prevent their interaction with

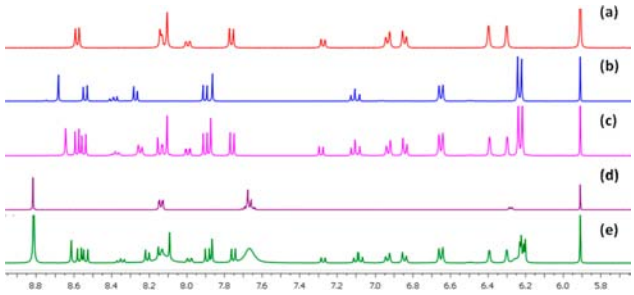

Figure 1. Partial ^{1}H NMR spectra (400 MHz, $C_2D_2Cl_4$, 298 K) of (a) **C1**, (b) **C2**, (c) **C1** + **C2**, (d) **C3**, and (e) a 1:1:3:1:1:1:1:1:1 mixture of **1**–**7** in the presence of $Zn(OTf)_2$ and $[Cu(MeCN)_4]PF_6$.

any zinc porphyrin. Despite the alert design, the conceived 3-fold completive self-sorting—as outlined in Scheme 1a—is not warranted *per se* because other ligands in the library, i.e., **2** and **3**, are able to bind to zinc(II) porphyrin **7**.[20] Fortunately, like simple anilines ($\log K \approx 2.20$),[20b] pyridine aldehyde **2** (see Figure S27) shows a much weaker binding than 4-iodopyridine (**5**) ($\log K \approx 3.43$)[20c] toward zinc(II) porphyrin. In fact, X-ray analysis of **C11** = [(**2**)(**7**)] (see Figure S50) shows a $Zn-N_{py}$ distance (3.01 Å) that is much longer than in any other pyridine–zinc(II) porphyrin coordination, while the $d(Zn-O_{aldehyde})$ of 4.90 Å argues against any interaction of the aldehyde oxygen and the zinc ion.[20b]

Using the optimized building blocks **1**–**7**, Cu^+, and Zn^{2+}, i.e., a nine-component library, we probed 3-fold completive self-sorting as depicted in Scheme 1a. As conceived, full orthogonality of all three complexes **C1**–**C3** was established, as indicated by ^{1}H NMR (Figure 1e). At this juncture, the use of two constitutionally dynamic iminopyridine ligands, instead of prototypical phenanthroline and terpyridine ligands,[10] adds a further degree of complexity and diversity[3b,5a] to the system. Because only three heteroassemblies are observed out of at least 126 possible homo- and heterocombinations (see SI), the degree of self-sorting[2d] M amounts to ≥42. The new 3-fold completive self-sorting is thus far more challenging than that in our previous eight-component system featuring $M = 11.7$.[10a]

As a next step, we decided to exploit the nine-component self-sorting for construing an unprecedented seven-component supramolecular scalene quadrilateral **QL** (Scheme 1c) that is superordinate to the known quadrilaterals (squares, rectangles, rhombuses, and trapezoids).[21] Integrative self-sorting of the three cornerstones **C1**–**C3** to **QL**, as depicted in Scheme 1a,c, demands that **C2** contributes twice to the requested four vertices. An alternative quadrilateral, equally with two **C2** corners (Scheme 3a), would arise if the **C2** motifs were

Scheme 3. (a) Two Possible Strategies in the Construction of Scalene Quadrilateral; (b) Chemical Structures of Ligands 14–16

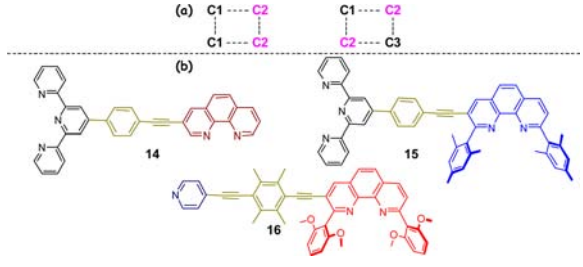

dx.doi.org/10.1021/ja410425k | J. Am. Chem. Soc. 2013, 135, 17743–17746

arranged in a diagonal fashion to each other and not adjacently (as in **QL**). Based on our prior experience,[10] we assessed the diagonal approach to be rather unfavorable, as it would risk formation of an undesired scalene triangle due to its lower entropic costs. Indeed, a 1:1:1:1:1:2 mix of the ligands **8**, **14**–**16** (Scheme 3), Cu^{+}, and Zn^{2+} furnished a mixture of both the scalene triangle $[ZnCu(\mathbf{8})(\mathbf{14})(\mathbf{16})](PF_6)(OTf)_2$ and scalene quadrilateral $[Zn_2Cu(\mathbf{8})(\mathbf{14})(\mathbf{15})(\mathbf{16})](PF_6)(OTf)_4$ (see Figures S45 and S46). Furthermore, in the diagonal approach there is the additional risk of generating constitutional isomers (see SI). Clearly, to fabricate a clean scalene quadrilateral, one has to be very precise in the choice of multifunctional ligands so that the formation of **C1** and **C3** units will bias the generation of the required two **C2** motifs in a cooperative manner.[22] We thus endowed the unsymmetrical bisphenanthroline **11** (Scheme 1b) with terminals **1** and **6** as well as the hybrid **10** with picolinaldehyde and pyridine spearheads, **2** and **5**, respectively. Both **10** and **11** are readily accessible via Sonogashira cross-coupling (see SI). Tetracarbaldehyde **9**, equipped with additional alkoxy groups to increase solubility, reflects twice the ligation properties of **4**. MM^{+} force-field computations on the scalene quadrilateral structure suggested that the known porphyrin–phenanthroline building block **8**[10a] may be well suited as the missing side.

To afford **QL**, all components (**3**, **8**–**11**, Zn^{2+}, and Cu^{+}) were mixed in a 5:1:1:1:1:2:1 ratio in CH_3CN/CH_2Cl_2 (4:1) and refluxed for 2 h. After obtaining a clear dark-violet solution, the reaction product was analyzed by spectroscopic techniques. To our delight, the ESI mass data established formation of the quadrilateral **QL** = $[Zn_2Cu(\mathbf{8})(\mathbf{11})(\mathbf{12})(\mathbf{13})](PF_6)(OTf)_4$ (Scheme 1c) by showing isotopically well resolved peaks for $[Zn_2Cu(\mathbf{8})(\mathbf{11})(\mathbf{12})(\mathbf{13})](OTf)_n^{(5-n)+}$ (n = 1, 2) at 1026.1 and 1417.6 Da (Figure 2).

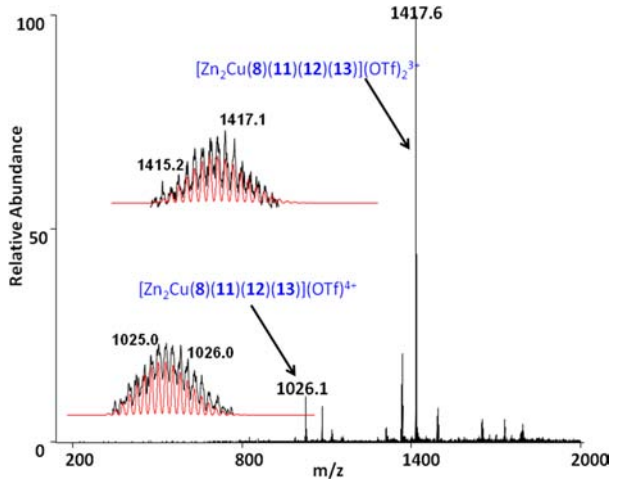

Figure 2. ESI-MS spectrum of **QL** (in CH_3CN) and experimental isotopic distribution (black lines) along with calculated isotopic distribution (red lines) for the species $[Zn_2Cu(\mathbf{8})(\mathbf{11})(\mathbf{12})(\mathbf{13})](OTf)_n^{(5-n)+}$ (n = 1, 2). Further signals are assigned in Figure S38.

A combination of ^{1}H NMR, ^{1}H–^{1}H COSY, and DOSY NMR (see SI) further corroborates the structural assignment of **QL**. Importantly, a comparison of the ^{1}H NMR spectra of **QL** and model complexes **C1**–**C3** provided strong support for the existence of $[Zn(\mathbf{8}_{phenAr2'})(\mathbf{12}_{diiminopy})]^{2+}$, $[Zn(\mathbf{11}_{phenAr2'})(\mathbf{12}_{diiminopy})]^{2+}$, $[Cu(\mathbf{11}_{phenAr2})(\mathbf{13}_{iminopy})]^{+}$, and $[(\mathbf{8}_{ZnPor})(\mathbf{13}_{py})]$ corners in **QL** (see Figure 3).[17b] For example, the

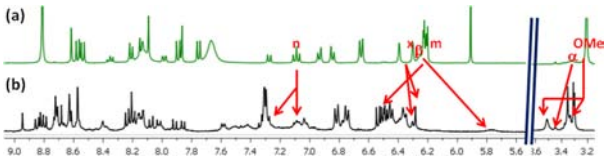

Figure 3. Partial ^{1}H NMR spectra (400 MHz, 298 K) of (a) 1:1:1 mixture of **C1** + **C2** + **C3** ($C_2D_2Cl_4$); (b) **QL** (CD_3CN). For the assignments of the NMR signals, see Scheme 1a.

$[(\mathbf{8}_{ZnPor})(\mathbf{13}_{py})]$ corner as the most labile binding motif in **QL** is established by the diagnostic 5.15 and 1.64 ppm upfield shift of pyridine protons α-H (δ = 3.44 ppm) and β-H (δ = 5.77 ppm) of ligand **10**, respectively. Furthermore, the resonances of the aldehyde protons of ligands **9** (δ = 10.2 ppm) and **10** (δ = 10.1 ppm) are absent in the ^{1}H NMR spectrum of **QL**, whereas new resonances at δ = 8.73, 8.63 (for **12**), and 8.40 ppm (for **13**) appear. The latter represent three constitutionally different imine protons and are diagnostic as they fall in the same spectral region as those of model complexes **C2** (d′-H, δ = 8.64 ppm) and **C1** (d-H, δ = 8.30 ppm, Scheme 1a).[14a] Analogously, mesityl protons (x/y-H and x′/y′-H) of ligand **11**, being enantiotopic in the free ligand, become constitutionally and diastereotopically different in **QL** due to the stereogenic unit $[Cu(\mathbf{11}_{phenAr2})(\mathbf{13}_{iminopy})]^{+}$.[10,14a] As a result, the resonances of the mesityl protons in **QL** (δ = 6.51–6.29 ppm) are split in four sets while showing a significant upfield shift compared to those in free **11** (δ = 6.96 and 6.98 ppm) due to the intimate stacking between the mesityl group of **11** and the iminopyridine units of the ligand **13**.[14a] Signals from the 2,9-bis(2,6-dimethoxyphenyl)-1,10-phenanthroline core, for example OMe protons (see Scheme 1a), yielded further structural information regarding the connectivity in **QL** at the $[Zn(\mathbf{8}_{phenAr2'})(\mathbf{12}_{diiminopy})]^{2+}$ and $[Zn(\mathbf{11}_{phenAr2'})(\mathbf{12}_{diiminopy})]^{2+}$ corners. Considering all molecular details, we expect eight singlets for the four methoxy groups in **QL** due to their constitutional difference and the stereogenic axis at copper(I) complex $[Cu(\mathbf{11}_{phenAr2})(\mathbf{13}_{iminopy})]^{+}$. Experimentally, five OMe singlets in a ratio 2:2:1:2:1 are observed at 3.30–3.51 ppm (cf. in **C2**: δ = 3.30 ppm), indicating that indeed two constitutionally different **C2** motifs are present in **QL**, the OMe groups of which are diastereotopic. Finally, a single diffusion coefficient obtained in the DOSY NMR ($D = 4.1 \times 10^{-10}$ m^2 s^{-1}) provides unambiguous evidence for the clean formation of **QL** as a single product. The derived radius r_{DOSY} = 15.6 Å (see Figure S33) is in good agreement with the computed one (r_{MM+} = 16.9 Å).

Differential pulse voltammetry (DPV) is a good tool to assess the environment of Cu^{+} ions, in particular because copper(I) ions show distinct oxidation potentials in HETPHEN and HETTAP settings.[10] Because the copper(I) oxidation wave in **C1** is located at 0.84 V_{SCE}, a single oxidation wave at 0.86 V_{SCE} is a strong support for a $[Cu(\mathbf{11}_{phenAr2})(\mathbf{13}_{iminopy})]^{+}$ motif in **QL** (see Figure S47). Imine bonds in **QL** are well corroborated by IR data, as the quadrilateral shows an absorption at 1597 cm^{-1} for the C=N stretching vibration, while **C1**[14a] and **C2** show vibrations at 1580 and 1586 cm^{-1}. According to the MM^{+} calculated structure, the four metal corners of **QL** are separated by 1.98, 1.50, 1.83, and 1.60 nm, taking the metal–metal distances as a measure (see Figure S51).

The clean one-pot synthesis of **QL** requires (1) full orthogonality of various complexation scenarios, i.e., HETPHEN, HETTAP, and pyridine–zinc porphyrin protocols; (2) constitutionally dynamic formation of terpy-like and bipy-

dx.doi.org/10.1021/ja410425k | J. Am. Chem. Soc. 2013, 135, 17743–17746

like[17b] ligand sites; (3) unsymmetric coordination at side **13** that guides the selective heterorecognition of two heteroleptic complexation scenarios at the opposing side **12**; and (4) proofreading for errors via reversible imine bonds and dynamic M←N coordination. Merging multiple similar and archetypically different interactions, such as those described in the present work, in the construction of multicomponent assemblies is the key to accessing structures of much higher complexity and to paving the way toward functional systems.

In summary, we report on the clean formation of the unprecedented seven-component scalene quadrilateral **QL** that conceptually evolved from a nine-component 3-fold completive self-sorted library (Scheme 1). Structural assignment and proof of purity were derived from a combination of various techniques, i.e., ESI-MS, ^{1}H NMR, DPV, DOSY-NMR, IR, and elemental analysis. In the light of other entities potentially forming from five ligands and two metals, the exclusive formation of **QL** is based on thermodynamic equilibration guided by 3-fold completive self-sorting and design criteria applied to ligands **8**−**11**. To the best of our knowledge, **QL** is the first supramolecular architecture that encompasses seven different components in its framework, thus demonstrating the power of multicomponent self-assembly.

■ ASSOCIATED CONTENT

Ⓢ Supporting Information

Experimental procedures and spectroscopic data for all new complexes and ligands; X-ray data for **C10** and **C11**. This material is available free of charge via the Internet at http://pubs.acs.org.

■ AUTHOR INFORMATION

Corresponding Author

schmittel@chemie.uni-siegen.de

Notes

The authors declare no competing financial interest.

■ ACKNOWLEDGMENTS

We are indebted to the Deutsche Forschungsgemeinschaft and the University of Siegen for financial support. We thank Dr. E. Neumann, Universität Siegen (X-ray structure of **C10** from CH_2Cl_2), and Dr. Jan W. Bats, Universität Frankfurt (X-ray structures of **C10** from CH_3CN and **C11**), for their support.

■ REFERENCES

(1) Groll, M.; Ditzel, L.; Löwe, J.; Stock, D.; Bochtler, M.; Bartunik, H. D.; Huber, R. *Nature* **1997**, *386*, 463.

(2) (a) Safont-Sempere, M. M.; Fernández, G.; Würthner, F. *Chem. Rev.* **2011**, *111*, 5784. (b) Osowska, K.; Miljanić, O. Š. *Synlett* **2011**, 1643. (c) Chakrabarty, R.; Mukherjee, P. S.; Stang, P. J. *Chem. Rev.* **2011**, *111*, 6810. (d) Saha, M. L; Schmittel, M. *Org. Biomol. Chem.* **2012**, *10*, 4651.

(3) (a) Lehn, J.-M. *Chem. Soc. Rev.* **2007**, *36*, 151. (b) Lehn, J.-M. *Angew. Chem., Int. Ed.* **2013**, *52*, 2836.

(4) Whitesides, G. M.; Grzybowski, B. *Science* **2002**, *295*, 2418.

(5) (a) Schmittel, M.; Mahata, K. *Angew. Chem., Int. Ed.* **2008**, *47*, 5284. (b) Wong, C.-H.; Zimmerman, S. C. *Chem. Commun.* **2013**, *49*, 1679. (c) Saha, M. L; De, S.; Pramanik, S.; Schmittel, M. *Chem. Soc. Rev.* **2013**, *42*, 6860.

(6) (a) Jiang, W.; Winkler, H. D. F.; Schalley, C. A. *J. Am. Chem. Soc.* **2008**, *130*, 13852. (b) Jiang, W.; Schalley, C. A. *Proc. Natl. Acad. Sci. U.S.A.* **2009**, *106*, 10425.

(7) Stang, P. J. *J. Am. Chem. Soc.* **2012**, *134*, 11829.

(8) (a) Christinat, N.; Scopelliti, R.; Severin, K. *Angew. Chem., Int. Ed.* **2008**, *47*, 1848. (b) Icli, B.; Solari, E.; Kilbas, B.; Scopelliti, R.; Severin, K. *Chem.—Eur. J.* **2012**, *18*, 14867.

(9) (a) Kishore, R. S. K.; Paululat, T.; Schmittel, M. *Chem. —Eur. J.* **2006**, *12*, 8136. (b) Smulders, M. M. J.; Jiménez, A.; Nitschke, J. R. *Angew. Chem., Int. Ed.* **2012**, *51*, 6681. (c) Li, S.; Huang, J.; Cook, T. R.; Pollock, J. B.; Kim, H.; Chi, K.-W.; Stang, P. J. *J. Am. Chem. Soc.* **2013**, *135*, 2084. (d) García, M. Á. A.; Bampos, N. *Org. Biomol. Chem.* **2013**, *11*, 27. (e) Li, L.; Zhang, H.-Y.; Zhao, J.; Li, N.; Liu, Y. *Chem.—Eur. J.* **2013**, *19*, 6498.

(10) (a) Mahata, K.; Saha, M. L; Schmittel, M. *J. Am. Chem. Soc.* **2010**, *132*, 15933. (b) Saha, M. L; Pramanik, S.; Schmittel, M. *Chem. Commun.* **2012**, *48*, 9459.

(11) (a) Schmittel, M.; Ganz, A. *Chem. Commun.* **1997**, 999. (b) Schmittel, M.; Kalsani, V.; Kishore, R. S. K.; Cölfen, H.; Bats, J. W. *J. Am. Chem. Soc.* **2005**, *127*, 11544.

(12) Schmittel, M.; Kalsani, V. *Top. Curr. Chem.* **2005**, *245*, 1.

(13) (a) Nitschke, J. R. *Acc. Chem. Res.* **2007**, *40*, 103. (b) Ronson, T. K.; Zarra, S.; Black, S. P.; Nitschke, J. R. *Chem. Commun.* **2013**, *49*, 2476. (c) Smulders, M. M. J.; Riddell, I. A.; Browne, C.; Nitschke, J. R. *Chem. Soc. Rev.* **2013**, *42*, 1728.

(14) (a) Schmittel, M.; Saha, M. L.; Fan, J. *Org. Lett.* **2011**, *13*, 3916. (b) Fan, J.; Saha, M. L.; Song, B.; Schönherr, H.; Schmittel, M. *J. Am. Chem. Soc.* **2012**, *134*, 150.

(15) Saha, M. L; Mahata, K.; Samanta, D.; Kalsani, V.; Fan, J.; Bats, J. W.; Schmittel, M. *Dalton Trans.* **2013**, *42*, 12840.

(16) (a) Leigh, D. A.; Lusby, P. J.; Teat, S. J.; Wilson, A. J.; Wong, J. K. Y. *Angew. Chem., Int. Ed.* **2001**, *40*, 1538. (b) Barboiu, M.; Dumitru, F.; Legrand, Y.-M.; Petit, E.; van der Lee, A. *Chem. Commun.* **2009**, 2192.

(17) (a) Saha, M. L.; Bats, J. W.; Schmittel, M. *Org. Biomol. Chem.* **2013**, *11*, 5592. (b) phenAr2 = 2,9-mesityl[1,10]-phenanthroline, phenAr2′ = 2,9-bis(2,6-dimethoxyphenyl)-1,10-phenanthroline, terpy = [2,2′;6′,2′]-terpyridine. and bipy = 2,2′-bipyridine.

(18) Schmittel, M.; Ganz, A.; Fenske, D.; Herderich, M. *J. Chem. Soc., Dalton Trans.* **2000**, 353.

(19) Krämer, R.; Lehn, J.-M.; Marquis-Rigault, A. *Proc. Natl. Acad. Sci. U.S.A.* **1993**, *90*, 5394.

(20) (a) Kirksey, C. H.; Hambright, P.; Storm, C. B. *Inorg. Chem.* **1969**, *8*, 2141. (b) Kojima, T.; Nakanishi, T.; Honda, T.; Harada, R.; Shiro, M.; Fukuzumi, S. *Eur. J. Inorg. Chem.* **2009**, 727. (c) Schmittel, M.; De, S.; Pramanik, S. *Angew. Chem., Int. Ed.* **2012**, *51*, 3832.

(21) Mahata, K.; Schmittel, M. *J. Am. Chem. Soc.* **2009**, *131*, 16544 and references cited therein.

(22) Hunter, C. A.; Anderson, H. L. *Angew. Chem., Int. Ed.* **2009**, *48*, 7488.